Research Journal of Applied Sciences, Engineering and Technology 4(15): 2283-2290, 2012
ISSN: 2040-7467

Submitted: October 23, 2011 Accepted: December 27, 2011 Published: August 01, 2012

Multifocus Image Fusion with PCNN in Shearlet Domain

Peng Geng, Xiang Zheng, Zhigang Zhang, Yujing Shi and Shiqiang Yan
Shijiazhuang Tiedao University, Shijiazhuang 050043, PR China

Abstract: The Shearlet form a tight frame at various scales and directions and are optimally sparse in representing images with edges. In this study, an image fusion method is proposed based on the Shearlet transform. Firstly, transform the image A and image B by the Shearlet transform. Secondly, PCNN is used for the every frequency subbands, which uses the number of output pulses from the PCNN's neurons to select fusion coefficients. Finally an inverse Shearlet is applied on the new fused coefficients to reconstruct the fused image. Some experiments are performed, comparing the new algorithm with the DWT, Contourlet and NSCT method based on the PCNN. The experiment results show that the proposed fusion rule is effective and the new algorithm can provide better performance in fusing images.

Keywords: PCNN, shearlet transform, NSCT

INTRODUCTION

The aim of image fusion is to integrate complementary as well as redundant information from multiple images to create a fused image output. Therefore, the new image fused should contain a more accurate information of the scene than any of the individual source images and is more suitable for human visual and machine perception or further image processing and analysis tasks. Image fusion technology has been applied in the remote sensing, medical image processing, automatic target recognition and computer vision and other fields. Fusion can be performed at different levels of information representation: in ascending order of abstraction, the pixel, feature and symbol levels. This study focuses on pixel-level fusion, which outputs gray-level images, serving to provide a visual display.

Recently, image fusion methods based on multiscale decomposition, as a very important fusion method, has been widely used in image fusion area and has achieved great success. The multiscale decomposition method of the image and the fusion rule are two critical factors in these method and directly impact on the effect of image fusion. Wavelet transform-based fusion approaches have been applied successfully in image fusion (El-Khamy *et al*., 2006). Although wavelets are good at isolating the discontinuities at edge points, smooth contours are missed. The Contourlet transform is a new analysis tool that aims at solving the two or higher dimensional discontinuities and it offers flexible multiresolution and directional decomposition for images. As a ''real'' representation of images, Contourlets proposed in by Do and Vetterli (2005) have been used in the fusion of infrared and visible light images. Nonsubsampled Contourlet Transform (NSCT), as a fully shift-invariant form of Contourlet, was proposed by Arthur *et al.* (2006) and leads to better frequency selectivity and regularity. A biological image fusion method based on NSCT by a variable-weight fusion rule is proposed by Tianjie and Yuanyuan (2011). But the NSCT is slow than other multiscale decomposition method. Shearlet proposed by Easley *et al*. (2009) a new approach provided in it, equipped with a rich mathematical structure similar to wavelets, which are associated to a multiresolution analysis. The Shearlet form a tight frame at various scales and directions and are optimally sparse in representing images with edges. In recent years, the theory of the Shearlet, which is used in image processing, has been studied gradually. Now the applications of Shearlets are mainly in image denoising, sparse image representation and edge detection. Its applications in image fusion are still under exploring.

The Pulse Coupled Neural Network (PCNN) is a recently developed artificial neural network model and it has been efficiently applied to image processing in applications such as image segmentation, image fusion, image recognition, Ruixing *et al*. (2008) presents an image fusion algorithms method based on PCNN and Biorthogonal Wavelet Transform (BWT). The multiscale fusion images were gotten by the parallel PCNN and the fused image can be obtained by Chai *et al*. (2010) proposed an image fusion algorithms method based on PCNN and NSCT. After a multiscale directional decomposition of NSCT, a new fusion method based on the PCNN is employed for the high frequency subbands, which uses the number of output pulses from the PCNN's neurons to select fusion coefficients. The subband coefficients corresponding to the most frequently spiking neurons of the PCNN are selected to recombine a new image.

In this study, a new improved model is proposed based on the PCNN in the Shearlet domain. After a multiscale directional decomposition of Shearlet, a new

Corresponding Author: Peng Geng, Shijiazhuang Tiedao University, Shijiazhuang 050043, PR China

fusion method based on the PCNN is used for the every frequency subbands, which uses the number of output pulses from the PCNN's neurons to select fusion coefficients. The subband coefficients corresponding to the most frequently spiking neurons of the PCNN are selected to recombine a new image. Finally an inverse Shearlet is applied on the new fused coefficients to reconstruct the fused image. Some experiments are performed, comparing the new algorithm with other multiscale decomposition fusion methods. The experimental results show that the proposed fusion rule is effective and the new algorithm can provide better performance in fusing image.

SHEARLET TRANSFORM

The basic theory of Shearlet transform is the composite wavelet theory which provides a kind of effective method for multiscale analysis by the affine system. In dimension n = 2, the affine system with the synthetic expansion character (Qiguang *et al.*, 2011) form is as follow:

$$A_{As}(\Psi) = \{\Psi_{j,k,l}(x)\} = \left|\det A\right|^{j/2} \Psi(S^l A^j x-k): \; j, l\in Z, k\in Z^2 \quad (1)$$

where, A, S are both 2×2 invertible matrices and |det S|=1. The matrix A^j correlates with the scale of transform correlation. S^l correlates with the geometric scale. The element of $A_{AS}(\Psi)$ is called composite wavelet, If $A_{AS}(\Psi)$ meet the following form of *Parseval* tight frame:

for $\forall f \in L^2(R^2)$, $\sum_{j,l,k}\left|\langle \psi\, j,l,k\rangle\right|^2 = \|f\|^2$

when, $A = A_0 = \begin{pmatrix} a & 0 \\ 0 & \sqrt{a} \end{pmatrix}$ and $S = S_0 \begin{pmatrix} 1 & 0 \\ 0 & 1 \end{pmatrix}$, it is called as Shearlet. A_0 is anisotropic dilation matrix. B_0 is shear matrix.

For $\forall\, \xi = (\xi_1, \xi_2) \in R$ and $\xi_1 \neq 0$, let $\hat{\Psi}^{(0)}(\xi)$ be given by:

$$\hat{\Psi}^{(0)}(\xi) = \hat{\Psi}^{(0)}(\xi_1, \xi_2) = \hat{\Psi}_1(\xi_1)\hat{\Psi}_2(\xi_1/\xi_2)$$

where, $\hat{\Psi}_1 \in C^\infty(R)$ is wavelet and $\hat{\Psi}_2 \in C^\infty(R)$, $\text{supp}\,\hat{\Psi}_1 \subset [-1/2,-1/16]\cup[1/16,1/2]$ and $\hat{\Psi}_2 \subset [-1,1]$. This implies $\hat{\Psi}^{(0)} \in C^\infty(R)$ and supp $\hat{\Psi}^{(0)} \in [-1/2, 1/2]$.

In addition, we assume that:

$$\sum_{j\geq 0}\left|\hat{\Psi}(2^{-2j}\omega)\right|^2 = 1, |\omega| \geq 1/8 \quad (2)$$

And for $\forall j \geq 0$

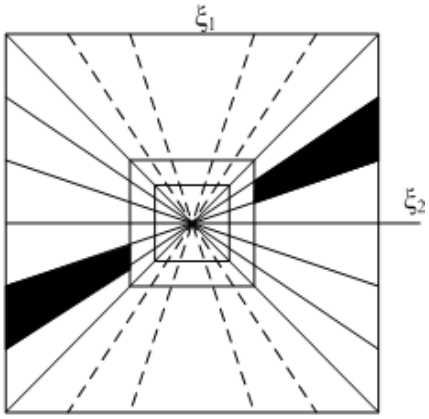

Fig. 1: The tiling of the shearlet in frequency domain

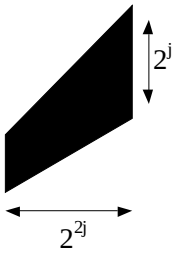

Fig. 2: The parabola scale of the shearlet transforms

$$\sum_{l=-2^j}^{2^j-1}\left|\hat{\Psi}(2^{-2j}\omega - l)\right|^2 = 1, |\omega| \leq 1 \quad (3)$$

Thus, it can be concluded from formula (2) and formula (3) that for $\forall\, (\xi_1, \xi_2) \in D_0$:

$$\sum_{j\geq 0}\sum_{l=-2^j}^{2^j-1}\left|\hat{\Psi}^{(0)}(\xi A_0^{-j} S_0^{-1})\right|^2 =$$

$$\sum_{j\geq 0}\sum_{l=-2^j}^{2^j-1}\left|\hat{\Psi}_1(2^{-2j}\xi_1)\right|^2$$

$$\left|\hat{\Psi}_2(2^j\frac{\xi_2}{\xi_1} - l)\right|^2 = 1$$

where, $D_0 = \{(\xi_1, \xi_2) \in \hat{R}^2 : |\xi_1| \geq 1/8, |\xi_2| \leq 1\}$, the function $\{\hat{\Psi} - - - (\xi A_0^{-j} S_0^{-j})\}$ forms a tiling of D_0 which is shown in Fig. 1. ξ_1, ξ_2 are the coordinate axes of the Shearlet transform in frequency domain. By the supporting conditions $\hat{\Psi}_1$ and $\hat{\Psi}_2$ the function $\Psi_{j,l,k}$ has the following domain support:

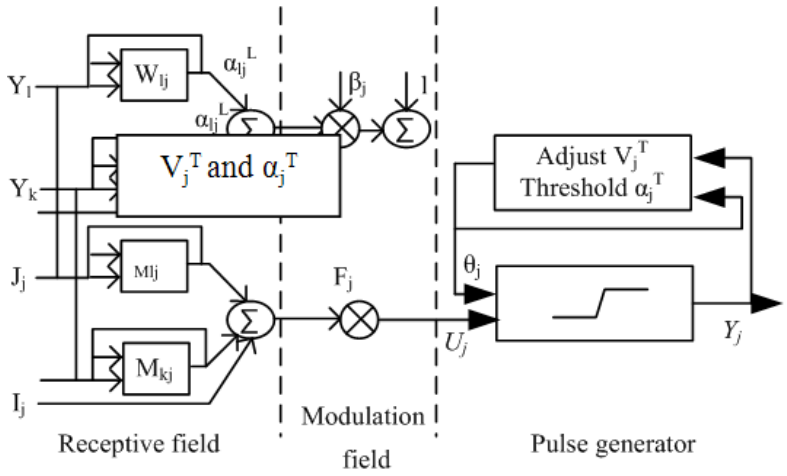

Fig. 3: The basic model of single neuronjin PCNN

$$\hat{\Psi}_1^{j,k,l(0)} \subset (\xi_1,\xi_2):\xi_1 \in [-2^{2j-1},-2^{2j-4}]\cup[2^{2j-4},2^{2j-1}],$$
$$\left|\frac{\xi_2}{\xi_1}+l2^{-j}\right| \le 2^{-j}$$

That is to say, $\hat{\Psi}_{j,l,k}$ is support on a pair of trapezoids, which the size is approximately $2^{2j}\times 2^{j}$ and oriented along lines of slope $l2^{-j}$. j is the scale of the Shearlet transform. This is shown in the Fig. 2. Similarly we can construct a *Parseval* frame $L^2(D_1)^\vee$ where D_1 is the vertical cone.

PULSE COUPLE NEURAL NETWORK

Principles of PCNN and its neuromime structure PCNN is a feedback network and each PCNN neuron consists of three parts:

- The receptive field
- Modulation field
- Pulse generator Ranganath *et al*. (1995)

The PCNN neuron's structure is shown in Fig. 3.

Principles of PCNN and its neuromime structure PCNN is a feedback network and each PCNN neuron consists of three parts: the receptive field, modulation field and pulse generator. The PCNN neuron's structure is shown in Fig. 3. In PCNN model, the neuron receives input signals from feeding and linking inputs through the receptive field. Then, input signals are divided two channels. Then, input signals are divided into two channels. One channel is feeding input F_j and the other is linking input L_j, where '$\otimes$' denotes convolution.I_j and J_j are the input stimulus such as the normalized gray level of image pixels.The interconnections M_{kj} and W_{kj} are the synaptic gain strengths for the feeding and the linking inputs, respectively, which dependent on the distance between neurons. α^F_{kj} and α^L_{kj} are the attenuation time constants. In the modulation field, the total internal activity U_j is the result of modulation. β_j is the linking strength and Y_j is the output of the neuron. The threshold θ_j changes with the variation of the neuron's output pulse. V^t_j and α^T_j are the amplitude gains and time constant of the threshold adjuster (Ranganath and Johonson, 1995; Johnson *et al*., 1999).

The mathematical model of the PCNN can be described as formula (4):

$$\begin{aligned} F_j &= \sum_k \left[M_{kj}\exp(-\alpha^F_{kj}t)\right]\otimes Y_k(t)+I_j \\ L_j &= \sum_k \left[M_{kj}\exp(-\alpha^L_{kj}t)\right]\otimes Y_k(t)+J_j \\ U_j &= F_j(1+\beta_j L_j) \\ \hat{\theta}_j &= -\alpha^T_j\theta_j+V^T_j Y_j(t) \\ Y_j(t) &= step(U_j-\theta_j) \end{aligned} \quad (4)$$

For each neuron, the feeding input is the intensity of the pixel corresponding to it. The linking input is the sum of the responses of the output pulses from surrounding neurons. A simplified model and discrete form described as formula (5) is used in this study:

$$\begin{aligned} F^k_{ij}(n) &= I^k_{ij} \\ L^k_{ij}(n) &= \exp(-\alpha_L)L^k_{ij}(n-1)+ \\ &V_L\sum_{a,b}W_{ij,ab}Y_{ab}(n-1) \\ U^k_{ij}(n) &= F^k_{ij}(n)*(1+\beta L^k_{ij}(n)) \\ \theta^k_{ij}(n) &= \exp(-\alpha_\theta)\theta^k_{ij}(n-1)+V_\theta Y^k_{ij}(n) \\ Y^k_{ij}(n) &= step(U^k_{ij}(n)-\theta^k_{ij}(n)) \end{aligned} \quad (5)$$

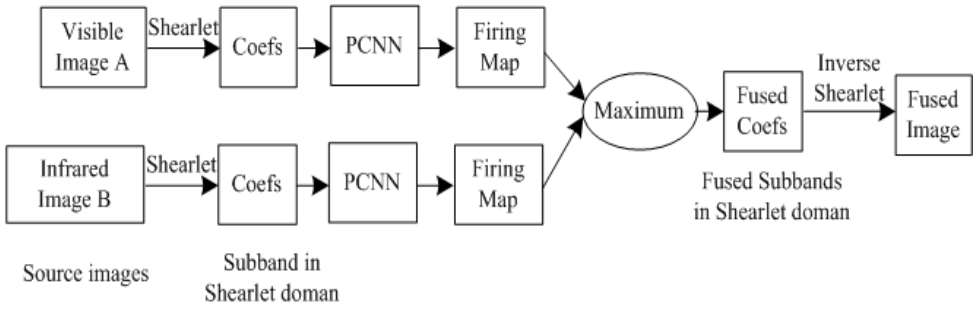

Fig. 4: Schematic diagram of shearlet-PCNN fusion algorithm

The *k*-th decomposed subband in the Shearlet coefficients is denoted by *k*. And the (*i*,*j*)-th pixel in the corresponding sub-image is denoted by subscripts *i* and *j*. The PCNN used for image fusion is two-dimensional array of laterally linked pulse coupled neurons on a single layer. The number of neurons in the network is in accordance with the number of pixels in the input image so as to form a one-to-one correspondence between the network neurons and the image pixels. Each pixel is connected to a unique neuron and each neuron is linked to the surrounding neurons.

THE PROPOSED FUSION ALGORITHM

The schematic diagram of the proposed Shearlet-PCNN algorithm is shown in Fig. 4 and implemented as:

- Transform the original images A and B using Shearlets, respectively, into one low-frequency sub-image and a series of high-frequency sub-images at L levels and k directions via Shearlets. The level of multiscale decomposition is 4.
- 2. Select fusion Shearlet coefficients from A and B via PCNN.
  - Let SH^K_A, SH^K_B, (k = 1, 2,...,) separately denote a series of coefficients of the original images A and B, decomposed to some level and direction via Shearlet Transform. Here, k denotes the *k*-th subband by Shearlet decomposition.
  - Take SH^K_A and SH^K_B separately as the feeding input to stimulate a corresponding PCNN.
  - Let $L^k_{ij}(0) = U^k_{ij}(0) = 0$, $\theta^k_{ij}(0) = 1$, $L^k_{ij}(0) = U^k_{ij}(0) = 0$ and $Y^k_{ij}(0) = 0$ in the *k*-th subband; i.e., each pixel does not fire.
  - Compute $L^k_{ij}(n)$, $U^k_{ij}(n)$, $Y^k_{ij}(n)$, $\theta^k_{ij}(n)$ according to Eq. (4) and Eq. (5)

  Firing times is calculated by:

$$T^{l,k}_{i,j}(n) = T^{l,k}_{i,j}(n-1) + T^{l,k}_{i,j}(n) \quad (6)$$

  - If n = Nmax, then iteration stops. Obtain the decision map $D^{l,k}_{i,j}$ by (7) and select the coefficients by (8), which mean that coefficients with large firing times are selected as coefficients of the fused image:

$$D^{l,k}_{F,ij} = \begin{Bmatrix} 1, if\ T^{l,k}_{A,ij}(n) \geq T^{l,k}_{B,ij}(n) \\ 0, if\ T^{l,k}_{A,ij}(n) \leq T^{l,k}_{B,ij}(n) \end{Bmatrix} \quad (7)$$

$$SH^{l,k}_{F,ij} = \begin{Bmatrix} SH^{l,k}_{A,ij},\ if\ \ D^{l,k}_{i,j} = 1 \\ SH^{l,k}_{B,ij},\ if\ \ D^{l,k}_{i,j} = 0 \end{Bmatrix} \quad (8)$$

where, $SH^{l,k}_{F,ij}$, $SH^{l,k}_{A,ij}$ and $SH^{l,k}_{B,ij}$ are the coefficients of the fused images F, A and B, respectively.

Reconstruct the new fusion image based on the new fused Shearlet coefficients by taking an inverse Shearlet transform.

EXPERIMENTS

To evaluate the performance of the proposed fusion method, experiments with fusion one set of multifocus images 'Clock' (512×512), Pepsi (512×512) and Book (480×480)

For comparison purposes, in this study, the fusion is also performed using the Contourlet-based method, NSCT-based method and Shearlet based method, in all of which the subband coefficients are fusion by the rule of formula (4) and (5) respectively. In Contourlet+PCNN NSCT+PCNN method and Shearlet+PCNN, the decomposition level is 4. Parameters of PCNN is set as p×q, $\alpha_L = 0.06931$, $\alpha_\theta = 0.2$, $\beta = 0.2$, $V_L = 1.0$, $V_\theta = 20$. The maximal iterative number is:
$N_{max} = 200$. W =

$$\begin{bmatrix} \sqrt{2} & 1 & \sqrt{2} \\ 1 & 0 & 1 \\ \sqrt{2} & 1 & \sqrt{2} \end{bmatrix}$$

The fusion results are shown in Fig. 5, 6 and 7.The Fig. 5a, 6a and 7a are the images focued on the right.

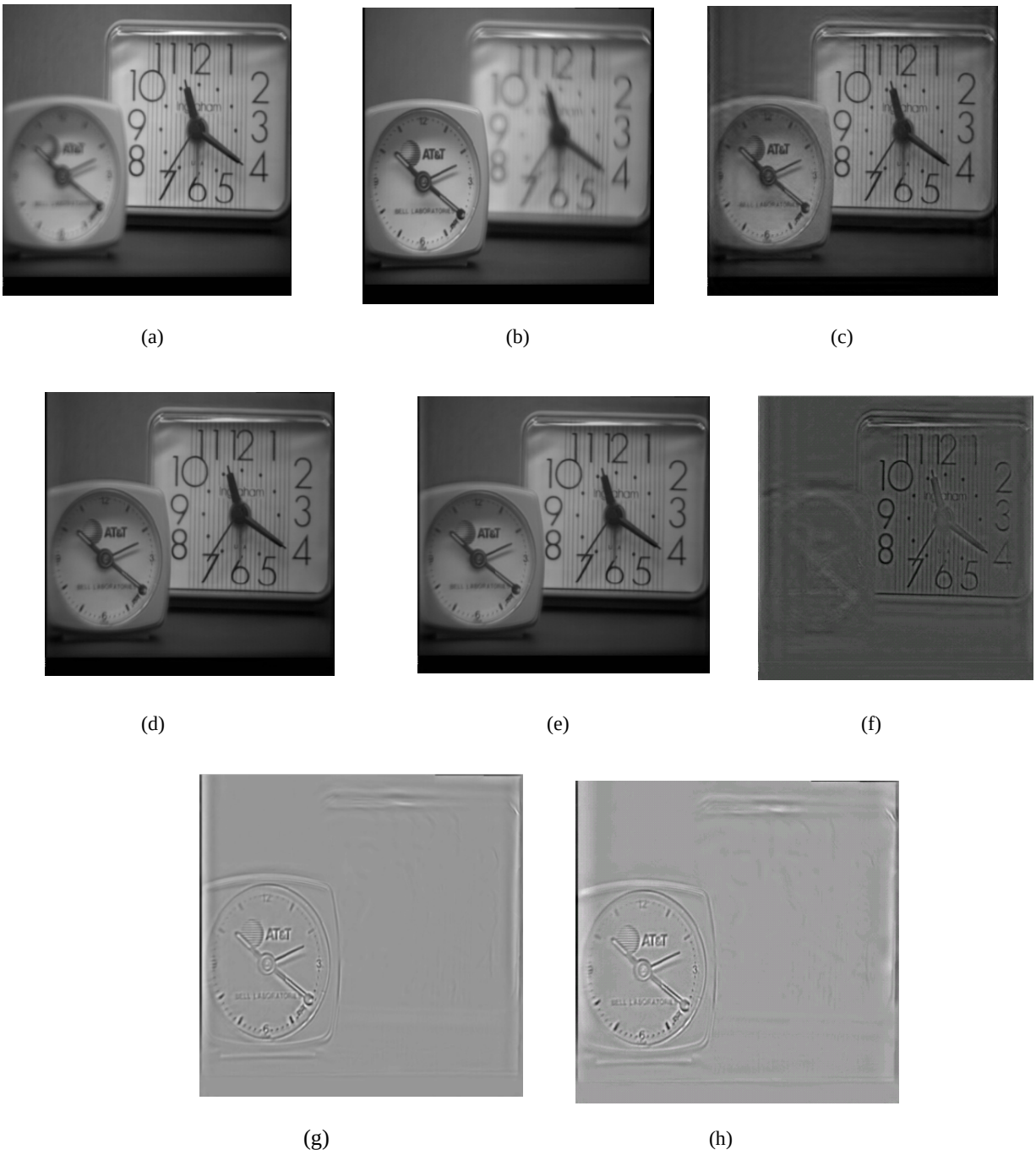

Fig. 5: The fusion results of 'Clock' image in different transform domain based PCNN

The Fig. 5b, Fig. 6b and Fig. 7b are the images focued on the left.

The fusion results are shown in Fig. 5c to e, Fig. 6c to e and Fig. 7c to e, which are, respectively, the fused images using Contourlet-PCNN, NSCT-PCNN and Shearlet-PCNN. From Fig. 5, 6 and 7 we can see that image fusing using Shearlets can obtain a fusion image clearly than other method. Fig. 5f to g, Fig. 6f to h and Fig.7f to h show the difference between fused images, which are fused results using Contourlet-PCNN, NSCT-PCNN and Shearlet-PCNN. Those indicates that Shearlet-PCNN extracts the better characteristic than other MSD-PCNN in multifocus images fusion.

For further comparison, two objective criteria are used to compare the fusion results. The first criterion is the Mutual Information (MI) metric proposed by Piella

Fig. 6: The fusion results of 'Book' image is in different transform domain based PCNN

(2003). The MI metric is employed here to objectively evaluate the performance of the PCNN methods in four different multiscale decomposition domain. This metric can demonstrate how much information the fused image conveys about the reference image. Thus, the higher the MI is, the better the result is. The MI is defined as:

$$MI(x_R; x_F) = \sum_{u=1}^{L}\sum_{v=1}^{L} h_{R,F}(u,v) \log_2 \frac{h_{R,F}(u,v)}{h_R(u)h_F(v)} \quad (8)$$

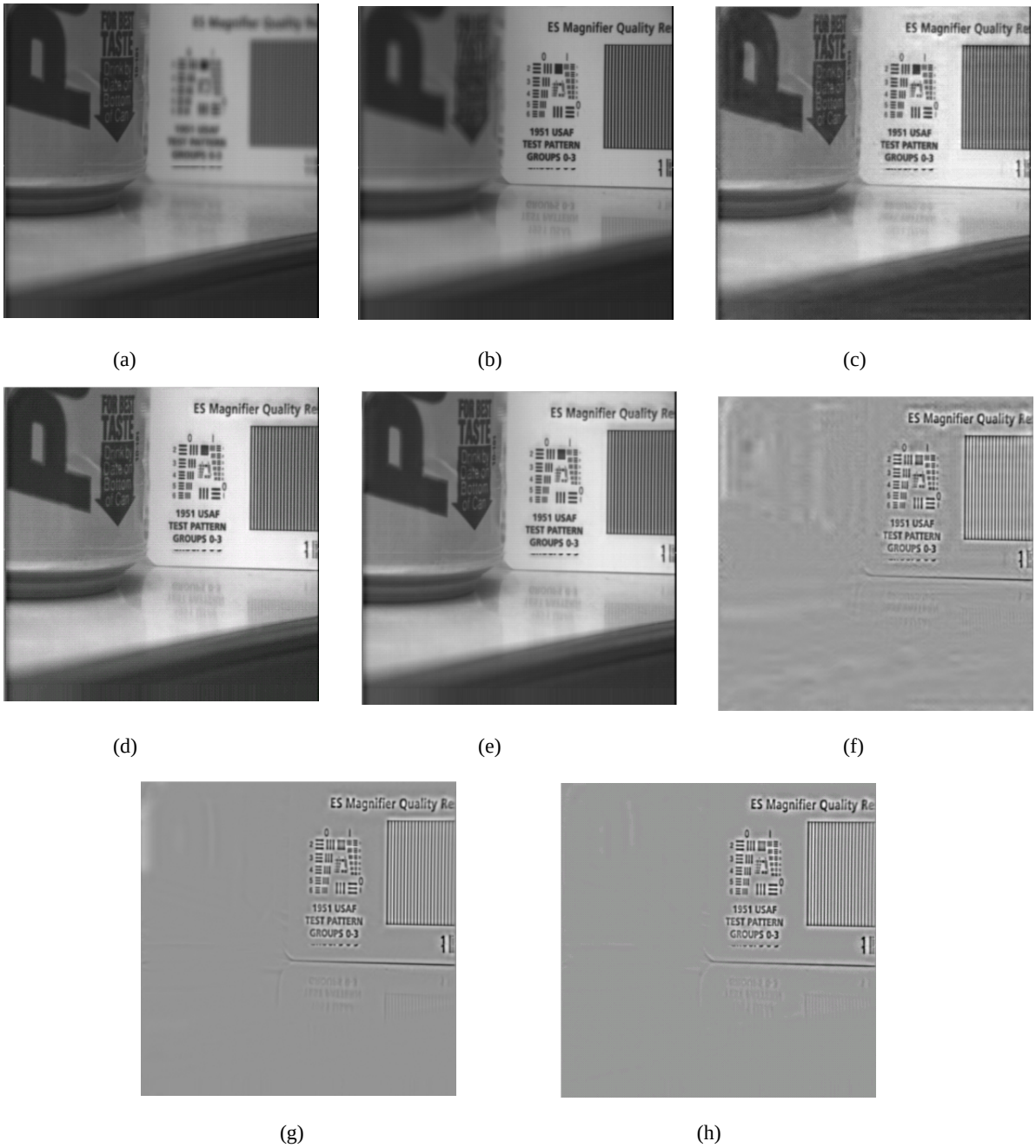

Fig. 7: The fusion results of 'Pepsi' image in different transform domain based PCNN

Where x_R and x_F denote the reference image and fused image, respectively, $h_{R,F}$ is the joint gray level histogram of x_R and x_F, h_R and h_F are the normalized gray level histograms of x_R and x_F and L is the number of bins. The MI values of the four different methods in Fig. 5, 6 and 7 are calculated and shown in Table 1. It can be seen from Table 1 that the MI value of the proposed method is the largest in the four methods and the MI value of the DWT method is the smallest. The results presented in this example can demonstrate that our approach can fuse the infrared image and visible image while retaining much more information than that of the other three methods.

The second criterion is the $Q^{AB/F}$ metric, proposed by Xydeas and Petrovic (2000), which considers the amount of edge information transferred from the input images to the fused images. This method uses a Sobel edge detector

Table 1: Performance of fusion in different transform domain based PCNN

Images	Criteria	Contourlt	NSCT	Shearlet
Clock	MI	5.6342	6.9674	7.1203
	$Q^{AB/F}$	0.5600	0.6796	0.6852
Pepsi	MI	5.7948	7.2841	7.3695
	$Q^{AB/F}$	0.6544	0.7137	0.7482
Book	MI	5.7879	6.8230	7.0980
	$Q^{AB/F}$	0.6539	0.7065	0.7109

to calculate the strength and orientation information at each pixel in both source image A, image B and fused image F.

The values of MI and $Q^{AB/F}$ of fusion results of the multifocus image fusion are listed in the Table 1. All the objective criteria prove that the fused image of the proposed method is strongly correlated with the source images and more image features, i.e., edges, are preserved in the fusion process, suggesting that the proposed method does well in the multifocus image fusion and outperforms Contourlet approach, NSCT and Shearlet approach based on in terms of $Q^{AB/F}$ and MI and provides the best performance in all kinds of images fusion.

CONCLUSION

The emergence and development of multiscale geometric analysis has led to new tools for image processing. The main advantage of Shearlets is that it can be studied within the framework of a generalized Multi-Resolution Analysis and with directional subdivision schemes generalizing those of traditional wavelets. The Shearlet is a 'true' two-dimensional MGA tool that captures intrinsic geometrical structure and it has been shown to be successful for many tasks in image processing such as image denoising, sparse image representation and edge detection. Furthermore, the method can yield more accurate reconstruction of images compared to NSCT and Contourlet. In this study, we presented a new fusion method based on the combination of the Shearlet transform and the PCNN. In this method, a PCNN-based fusion rule was employed to make a decision on selecting the Shearlet coefficients for high frequency and low frequency subbands. The subbands coefficients corresponding to the most frequently spiking neurons of the PCNN were selected in image fusion. The results of experiments of multifocus image fusion demonstrate the effectiveness of our proposed method by the objective criteria and the visual appearance.

ACKNOWLEDGMENT

The authors would like to thank Dr. Qu Xiaobo for his help in the understanding and application of the PCNN and provided images. Some of the images are available from http://www.imagefusion.org. This study was supported in part by University Science Research Project of Hebei Province under grant 2011142 and the Natural Science Foundation ofShandong Province under grant ZR2011FM004.

REFERENCES

Arthur, L., D. Cunha and J. Zhou, 2006. The nonsubsampled Contourlet transform: Theory, design and application. IEEE T. Image Proc., 10(15): 3089-3101.

Chai, Y., H.F. Li and J.F. Qu, 2010. Image fusion scheme using a novel dual-channel PCNN in lifting stationary wavelet domain. Optics Commun., 283(19): 3591-3602.

Do, M.N. and M. Vetterli, 2005. The Contourlet transform: An efficient directional multiresolution image representation. IEEE T. Image Proc., 14(12): 2091-2106.

Easley, G.R.,D. Labate and F. Colonna, 2009. Shearlet-based total variation diffusion for denoising. IEEE T. Image Proc., 18(2): 260-268.

El-Khamy, S.E., M.M. Hadhoud, M.I. Dessouky, B.M. Salam and E.S. Abd, 2006. Wavelet fusion: A tool to break the limits on LMMSE image super-resolution. Inter. J. Wavelets Multiresolution Inf. Proc., 4(1): 105-118.

Johnson, J.L., M.L. Padgett andO. Omidvar, 1999. Overview of pulse coupled neural network special issue. IEEE T. Neural Network., 10(3): 461-463.

Piella, G., 2003. A general framework for multire solution image fusion: From pixels to regions. Inf. Fusion, 4(4): 259-280.

Qiguang, M., S. Cheng, P. Feixu and Y. Mei, 2011. A novel algorithm of image fusion using Shearlets. Optics Commun., 284(6): 1540-1547

Ranganath, H., S. Kuntimad and J.L. Johonson, 1995. Pulse coupled neural networks for image processing. Proceedings of the IEEE Southeastcon '95 Conference, March 26-29, 1: 37-43.

Ruixing, Y., Z. Bing and Z. Ke, 2008. New image fusion algorithm based on PCNN and BWT. Guangdianzi Jiguang/. J. Optoelectronics Laser, 19(7): 956-959.

Tianjie, L. and W.Yuanyuan, 2011. Biological image fusion using a NSCT based variable-weight method. Inf. Fusion, 12(2): 85-92.

Xydeas, C.S. and V. Petrovic, 2000. Objective image fusion performance measure. Electronics Letters, 36(4): 308-309.